MRI and DTI in Clinical Neurosurgery

Lauren O'Donnell

December 19, 2005

1 Introduction

This document attempts to describe the clinical practice of neurosurgery from the point of view of a computer scientist/medical engineer. I will focus on the current use of imaging technology in clinical practice and on the potential utility of diffusion tensor MRI imaging (DTI). The two main questions I have tried to answer are "How do doctors actually use MRI for neurosurgery?" and "What do doctors want to know that DTI might tell them?"

This document was produced as part of MIT's HST 203, Clinical Experience in Medical Engineering and Medical Physics. Over a period of three months in the fall of 2005, I shadowed Dr. Alexandra Golby (Assistant Professor, Department of Neurosurgery, Harvard Medical School) while she saw patients in her weekly neurosurgery clinic at Brigham and Women's Hospital in Boston, MA. I attended many of her research group meetings, I attended an Epilepsy Board meeting, and I observed two neurosurgeries.

In addition to the shadowing component, the project had a technical component. I produced 3D visualizations of the white matter of several subjects by clustering paths from DTI tractography, then grouping clusters by anatomical region. To my knowledge, this is the first time fiber clustering has been applied to neurosurgical visualization. I evaluated the utility of the visualizations with Dr. Golby, and here I present the "second try," images that include some of the additional features she found necessary.

The rest of this document is organized as follows: First I describe the clinical shadowing part of the project, focusing on how MRI was used in the situations I observed. This is followed by background on Diffusion Tensor MRI and a discussion of how Dr. Golby would like to be able to use this information. Finally I present visualizations of two surgical patients.

2 MRI Use in Neurosurgery

MRI is extremely important in the neurosurgery clinic. There is a dark room with lightboxes and computers just like in a radiology department, and this room is where the doctors are when they are not seeing a patient. Before seeing a patient the scans are reviewed, often in concert with other specialists such as

radiation oncologists or other neurosurgeons. In general I was amazed by the sheer number of images for every patient, but also by the lack of any "fancy computer science technology" in the clinic. In fact, the main technical difficulty for physicians was learning the variety of programs for displaying MRI images that come on CDs.

All image viewing that I saw used the standard two-dimensional slices which doctors are trained to read, as opposed to the fancy spinning three-dimensional brains that we as computer scientists are more accustomed to. I was surprised that even though surgery is fundamentally three-dimensional, trained surgeons prefer two-dimensional information. This began to make sense, however, when Dr. Golby explained that in a three-dimensional scene, she can't tell what is "in the slice" and what is "in front of it." Obviously she needs to know exactly where the anatomy is, and the two-dimensional images are not ambiguous in this way.

MRI in neurosurgery is fundamentally an aid for making decisions. In the rest of this section I will describe how MRI has been used for making decisions in the types of situations that I have observed in the clinic and operating room. I have grouped these into five main sections: tumors, hydrocephalus/shunt maintenance, arteriovenous malformation or bleeding, neurosurgical planning, and neurosurgery.

2.1 Clinical Situation 1: Tumors

One of the most important decisions that must be made when a tumor is found is how to treat it. Treatment options include "watch and wait," biopsy, surgery, stereotactic radiosurgery (one large dose at once), stereotactic radiotherapy (smaller doses over a few sessions, for the case when the tumor is large or near sensitive regions such as the optic nerve or chiasm), and chemotherapy (which may be combined with other treatments). The choice of treatment is influenced by several factors: a) the type of tumor, b) the rate of growth of the tumor, c) the size of the tumor, d) the location of the tumor, and e) the symptoms and current quality of life of the patient.

MRI is used to evaluate factors a) through d). The tumor type is diagnosed based on its appearance and location, using knowledge from years of clinical experience. For example in the case of one patient, the relevant question for diagnosis was "Is this metastatic cancer or possibly MS?" because both could appear as hyperintense regions on MRI. In another patient, there appeared to be a tumor of the pineal gland on MRI which was then confirmed based on a positive history for recent inability to sleep. Another patient had a large tumor located at the brain surface in MRI images. This was diagnosed as a meningioma, a tumor of the meninges which cover the brain, based partially on its location (though later I learned that meningiomas can occur in the ventricles as well).

The rate of growth of a tumor is evaluated using MRI scans from different points in time. A patient with a small, slow-growing, or recently discovered tumor might be in the "watch and wait" category. In this case, the tumor is

Tumor Type	%	Description
Glioma	50%	From glial cells, supporting cells for neurons This is a broad category with a wide range of malignancy.
Meningioma	15%	From meninges that cover the brain and spinal cord
Pituitary	10%	Located in pituitary gland (may secrete hormones)
Pineal	1%	Located in pineal gland
Metastatic		Originates elsewhere in the body
Lymphoma		Primary tumor, or rarely secondary (metastatic)

Table 1: Common Tumor Types in Adults (percentages from [1])

MRI Sequence	Use	Recognition Tip
T1	anatomical	CSF dark; fat, white matter bright
T2	lesion often bright	CSF bright; fat, white matter dark
FLAIR	lesions bright	CSF dark, white matter dark
Contrast	blood-brain barrier	Bright in sinuses and choroid plexus and in most malignant tumors

Table 2: MRI Sequences

measured on two or more MRI scans (using the latest images and prior ones), and a decision is made as to whether it seems to be growing. The measurement is done by drawing a line with the mouse across the widest dimension, and possibly perpendicular to that as well. Depending on the result, the patient might need surgical treatment, or if not, would be asked to return with another scan after 3 months, 6 months, or a year.

Common types of tumors and their characteristics are listed in Table 1. Malignancy in brain tumors is defined not by whether they metastasize, since this does not happen with primary brain tumors, but rather by how quickly they grow and by their cellular differentiation as measured by pathology (whether the cells look normal or have many mitoses, etc.). However tumors in other parts of the body can metastasize to the brain.

Various MRI sequences are used to elicit information about a tumor. Table 2 lists the ones that seemed to me to be the most used, as well as tips for recognizing that type of image.

2.1.1 Tumor Follow-Up Care

Most of the tumor patients that I met were actually in the clinic for follow-up. This showed me how successful neurosurgery is. In general, MRI was used to check for recurrence of tumors.

2.2 Clinical Situation 2: Hydrocephalus/Shunt Maintenance

A shunt consists of a catheter which is inserted into the lateral ventricles, a valve, and a catheter that drains into either the peritoneum or the right atrium. In the case of a programmable shunt, a magnetic device is used to adjust the opening pressure of the valve. This is done in the clinic and must be performed after every MRI since the shunt can be reset in a magnetic field. The current opening pressure is read using a skull x-ray, and the image of the valve looks sort of like a clock with 2 (large and small) circles to give its orientation. The valve can be felt through the skin on the back of the head. On a CT scan, the shunt catheter appears as a very bright, thick line in a lateral ventricle.

I saw one patient who was in the clinic for follow-up of an emergency shunt revision (that is what they call an operation to fix an existing shunt). In addition, I saw another patient who was a candidate for a shunt. This patient was an elderly woman who had enlarged ventricles seen on MRI, with the symptoms of normal pressure hydrocephalus (NPH), a triad which includes urinary incontinence, difficulty walking, and dementia. NPH is one of the few reversible causes of dementia in the elderly, because it can be reversed if the ventricles are drained. Before surgery, an inpatient test is done to determine if CSF drainage reduces symptoms: a lumbar catheter is inserted to drain CSF gradually over a few days, and if the symptoms improve the patient is a good candidate for a shunt. Interestingly, Dr. Golby informed me that it is not known why or how that particular triad of symptoms is caused by NPH, but stretching of frontal white matter tracts is implicated.

2.3 Clinical Situation 3: Arteriovenous Malformation or Bleeding

I saw two patients that fell into this category. One patient had surgery to remove an arteriovenous malformation that had caused one seizure. The other patient had been referred to the neurosurgeon due to an event in the past year where bleeding in the brainstem area had caused diplopia. In both cases the MRI was inspected for vascular abnormalities.

2.4 Clinical Situation 4: Neurosurgical Planning

I learned about planning for two types of neurosurgeries, radiation therapy and standard surgery. In stereotactic radiosurgery, the general idea is to aim beams of radiation into the skull from many directions, such that the beams converge to produce a high dose only inside of the tumor. There are multiple types of radiosurgery machines, most of which require stereotactic frames to fix the head in place, and one which is called the CyberKnife which automatically detects head position. Planning for radiation therapy involves defining the tumor location and pinpointing the location of sensitive regions which include the optic

nerve and chiasm. This information is then analyzed by treatment planning software.

The conversations I have had with Dr. Golby about planning for conventional neurosurgery focused mainly on current and potential uses of DTI. This information is included later in this document, in sections 3.2 and 4.

2.5 Clinical Situation 5: Neurosurgery

I observed two neurosurgeries. The first one was actually prior to the official start of this project. In this case I saw the beginning of the surgical process, including head fixation with a frame, registration of presurgical MRI data, and cortical stimulation for language mapping. The presurgical MRI was registered by touching points on the face and scalp with a surgical probe, which then were aligned with the head surface from the scan. The mapping was done by asking the patient to count, then stimulating in different regions to find those which caused his speech to waver or stop. There were also epilepsy doctors present and cortical electrodes were used to test for seizures. The EEG was visible on a screen next to the patient.

The next neurosurgery was a trans-sphenoidal resection of a non-secreting pituitary tumor. The approach in this type of surgery is through the nose, through the sphenoid sinus, and through the sella turcica (the bony cavity at the skull base where the pituitary gland is located). The sella is separated from the rest of the brain by a membrane, the diaphragma sellae, so the brain is still separated from the sinuses after the surgery. The sphenoid sinus borders the optic nerve and interior carotid which must be avoided. In this surgery, both an endoscope and a surgical microscope were used. Both produced clear images of the surgical field, but the endoscope could be inserted into the sinus and therefore had a wider field of view; however it could not be locked in place like the surgical microscope. Surgical navigation was aided by CT images and the VTI/GE surgical guidance device. Image registration was done by means of a light plastic stereotactic headpiece which was worn during the scan and replaced in the same position before surgery. Specific points on the headpiece were touched with the surgical probe in order to register the images to the patient. Then during surgery, the surgical probe was inserted into the sinuses periodically, to check the depth and trajectory towards the tumor. This surgery was amazing because using the surgical microscope it was not possible to see into the sella turcica, so Dr. Golby spent hours patiently removing all possible tumor from the (unseen) cavity using very small "scraping" tools which were on the end of long, thin handles.

3 The Potential Role of Diffusion MRI

Diffusion MRI is the first noninvasive technique for measuring white matter fiber structure in vivo. Thus it has begun to see use in neurosurgical planning and guidance [5, 13, 10, 4]. The majority of the cited studies focus on

three-dimensional reconstructions (approximations) of the fiber tracts through a process called tractography, while one article describes tumor appearance on two-dimensional images that use color to show tract orientation. It should be noted that unlike all previously available types of MRI images, a single DTI image slice is fundamentally not two-dimensional because at every voxel location, there is an estimate of diffusion in three dimensions.

In this section I briefly give background information on DTI data, then I present a description of how Dr. Golby would like to be able to use the information from DTI, with a list of her specific application suggestions. Finally I will present information from the literature on DTI in neurosurgery.

3.1 DTI Background Information

Diffusion MRI measures the diffusion of water molecules. The amount of diffusion can be measured in any direction, and by choosing many evenly distributed directions, one can build up a 3D model of diffusion magnitude. This is useful in tissues with a strong orientation like white matter or muscles, because the amount of diffusion in each direction is determined by the tissue structure. The exact cause is unknown, but in the brain higher diffusion is measured parallel to white matter fiber tracts than perpendicular to them, so diffusion measurements can be used to give a local fiber coordinate system. The simplest representation of the shape of diffusion in 3D is the diffusion tensor, a 3x3 symmetric, positive-definite matrix whose major eigenvector points in the principal diffusion direction (direction of the highest diffusion). The principal eigenvector will not always match an underlying fiber tract direction (for example in the ventricles there are no fiber tracts yet diffusion can be measured) but if the largest eigenvalue is much larger than the last two eigenvalues, this is good evidence for the presence of a tract.

Tensor anisotropy measures are ratios of the eigenvalues that are used to quantify tensor shape. Three intuitive measures are c_L, c_P, and c_S, the linear, planar, and spherical shape measures. They describe whether the shape of diffusion (and the local tissue structure) is like a cigar (linear), pancake (planar), or sphere (spherical). The linear shape measure is defined as $\frac{\lambda_1-\lambda_2}{\lambda_1}$ (where the normalization in the denominator can instead be the tensor norm) [12]. The linear measure is a good indication of the presence of a fiber tract. For this purpose, the fractional anisotropy (FA), a normalized variance of the eigenvalues, may also be used. However the FA is less specific for indicating the presence of a fiber tract as it can be high in areas of planar diffusion which can indicate tract crossings or branchings [2].

DTI may be visualized in two or three dimensions, depending on the subset of the data that is presented. An example of 2D and 3D visualization is found in Figure 1. These images (and the rest of the images in this document) were generated with the DTMRI module in the 3D Slicer (software that I wrote in conjunction with the Lab for Mathematics in Imaging at BWH) along with additional matlab code for tract clustering. On the left side of Figure 1, the top image is a zoomed-in part of a semi-transparent coronal anisotropy image,

showing glyphs representing the major eigenvector in each voxel (technically these glyphs are displayed in 3D but as their out-of-plane component is hard to see it's essentially a 2D image). The two images in the lower left display the color scheme commonly used to represent the orientation of the major eigenvector: blue is superior-inferior, red is left-right, and green is anterior-posterior [8]. The brightness in these images is controlled by tensor anisotropy, which can be seen without orientation color information in the lower right image.

On the right side of Figure 1 the top image contains tractography in a DTI dataset. The paths (variously and somewhat incorrectly referred to as "tracts" or "fibers" in the literature and in this document) were interpolated through the major eigenvector field of the DTI data, in this case with second order Runga-Kutta integration. The different colors were assigned automatically by a whole brain tract clustering process [7] and a subset of the clusters was selected to create this image.

3.2 Neurosurgical Description and Application Suggestions from the Neurosurgeon

In this section I relate, to the extent that I have understood it, the point of view of a neurosurgeon relative to DTI and the brain.

Surprisingly, I have learned that the unfixed brain has a consistency not dissimilar to Jello. It is "suckable." The white matter fibers are not visible in any way, but the consistency of a tumor is different and can be more fibrous. During surgery, electrical stimulation is used to interrupt neural function (speaking, counting, movement) in order to assess proximity to eloquent regions. These are as opposed to "silent" regions whose function is harder to measure. This stimulation is done on the cortex, not in the white matter, so it does not directly provide information on which white matter regions are functional.

While the electrical stimulation is obviously an invaluable method, it could be helpful to have additional information about the structure of the white matter in the region of the lesion. Dr. Golby has suggested methods of presenting the information in a DTI scan that would be useful to her, the majority of which have not been tried before to my knowledge. Despite her general preference for 2D images, she is in fact interested in 3D visualizations of fiber tracts, although at this point she is not sure to what extent they should be trusted. Currently she finds the 2D images with superimposed glyphs to be the most useful in surgical planning. Her suggestions are discussed below and are summarized in Table 3.

Her first idea relates to the general concept that doctors analyze brain images by comparing the left and right side to look for abnormalities, and it is not clear how to do that with three-dimensional information from tractography. Dr. Golby suggested that color-coding corresponding tracts on the right and left sides would facilitate this comparison. This is not a simple request as it depends on having either anatomical labels for the tracts or an algorithm for matching them across hemispheres.

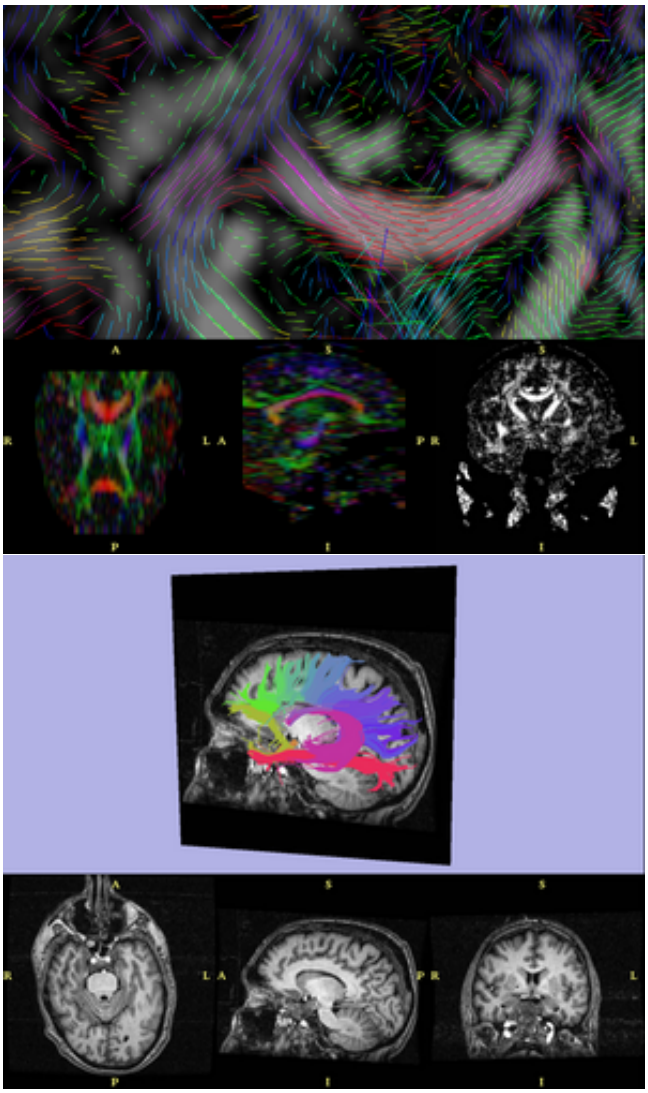

Figure 1: Two- and three-dimensional DTI visualization (in two different subjects)

The second two items in Table 3 have to do with the 3D information being unclear. ("What is in front/behind/inside the tumor?") In the 3D Slicer visualization system, it is possible to make a surface model of the tumor semi-transparent to see what is inside, but then it is not possible to differentiate whether a tract is inside or behind the tumor. Similarly, when viewing tracts in 3D along with 2D image slices, the 3D extension of the path visually occludes its intersection with the 2D slice and therefore with the tumor. So one suggestion is to augment the 3D view of the tracts by coloring them where they pass through the tumor. Another possibility is to show the paths in the 2D slices instead.

The fourth item in Table 3 was extremely interesting. When neurosurgeons make the initial incision, they try to make it parallel to white matter fibers in order to cut as few as possible. They do not "scoop" out a cavity, but rather cut a line in the surface and then follow that direction inward. The orientation of this line on the surface is determined by the known anatomical orientation of the fibers, however this is not patient-specific and may not be correct in all cases. Dr. Golby pointed out that this orientation may vary in neuroanatomical illustrations, as in for example the fibers in Meyer's loop around the inferior horn of the lateral ventricles, where an incision is made to approach tumors of the ventricles. So she would like to somehow see which way the fibers are going below the surface, in order to plan the orientation of the incision.

The last item in Table 3 relates to the fact that the fibers displayed using tractography are most assuredly not representations of individual axons (with a scale of microns), but rather are paths which follow the most probable fiber orientations measured on a scale of millimeters using diffusion MRI. Due to noise, partial voluming, or fiber crossing, tractography makes anatomical errors, and it is important to a) display only paths that pass quality thresholds and b) provide a visual quality estimate.

	Application Suggestions from Dr. Golby
1	Color code matching tracts on right and left.
2	Color the part of the tract that is inside the tumor.
3	Show the tracts on the 2D images.
4	Show the fiber orientation for incision planning.
5	Show how certain it is that the tract exists.

Table 3: Neurosurgical DTI Wish List

3.3 DTI In Tumors

The main potential use of DTI in neurosurgery is to evaluate whether functional white matter is present in a tumor. However, DTI doesn't measure function, it measures structure, and it is not a simple problem to correlate DTI anisotropy measures and principal directions with white matter functionality. However, by assuming that function is preserved in white matter that looks "normal" on

DTI, methods have been suggested for assessing the integrity of fiber tracts.

Using DTI color images the following categories have been introduced to describe white matter tracts in the vicinity of a tumor: displaced, edematous, infiltrated, and disrupted [13, 3]. Their categorization was performed in the following way: Displaced tracts were said to be those with normal anisotropy but abnormal location or orientation. Edematous tracts looked normal (orientation and anisotropy) in the DTI color images but had high T2 intensity. Infiltrated tracts were those which had reduced anisotropy but could be identified with DTI color images. Finally, disrupted tracts were classified as such if they could not be identified on the DTI color images.

In addition to the clinical application of DTI colormaps, various groups have employed tractography to visualize the relationship between tumors and white matter [5, 10, 4]. In one recent paper, intraoperative tractography was used to visualize and quantify the shifting of white matter fibers (primarily the pyramidal tract but in one case the corpus callosum) that occurs during surgery [5]. This study found average shifts of 2.7 mm, with a range from -8 to +15mm, where negative and positive numbers indicate movements toward and away from the craniotomy opening, respectively.

4 Two Surgical Cases, Illustrated Using Advanced Visualization Tools

I created retrospective visualizations of two surgical cases in which tumors had been resected by Dr. Golby. Each case had presurgical data including T1- and T2-weighted MRI, DTI, and fMRI.

Creation of the visualizations had several steps. The first step was whole-brain tractography, using a c_L threshold to define the region of interest for seeding and a c_L threshold for the anisotropy cutoff (where fiber tracking stops). The optimal thresholds for clustering applications are under investigation but the range I have used for seeding is in general 0.2 to 0.35 minimum c_L, and for stopping 0.15 to 0.25 c_L. The minimum path length was 40mm. The second step in production of the visualizations was an automatic clustering of the paths from tractography which produced approximately 120 bundles using spectral clustering as in [7]. The clustering step was followed by an interactive manual anatomical labeling. While developing this interactive tool in the 3D Slicer program, I performed anatomical labeling with repeated reference to the white matter anatomy described in [6, 3, 11].

4.1 Case 1

Patient 1, a 54 year old male, presented with a seizure and word finding difficulty, and on MRI had a large left temporal mass. The tumor was resected and the pathologic diagnosis was anaplastic oligoastrocytoma, WHO Grade III. During surgical resection in the posterior region, the patient had difficulty with speech;

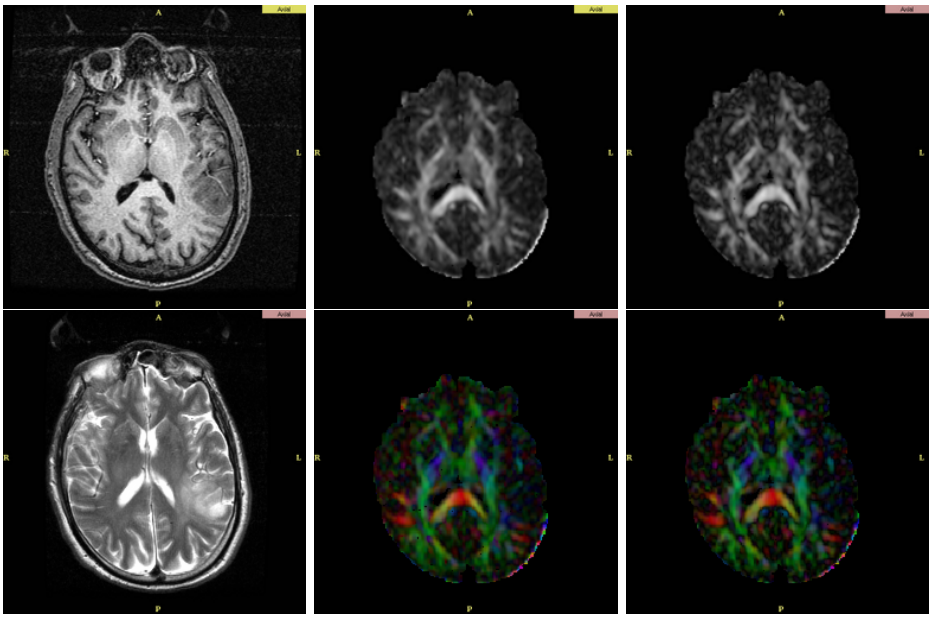

Figure 2: Two-dimensional DTI visualization of patient 1. First row: MPRAGE, FA, c_L. Second row: T2, DTI colormap (brightness by FA), DTI colormap (brightness by c_L). The window and level for the FA and c_L images was set to be window of 1 and level of 0.5 to allow direct image comparison.

superiorly, electrical stimulation interrupted language function. About half of the tumor was resected while the rest was left to preserve function.

Figure 2 shows a standard 2D slice visualization at one axial location for patient 1. The DTI colormaps would seem to indicate that tracts are not present in this level of the tumor, due to the lack of anisotropy, according to references [13, 3]. However there are some bright spots in the tumor region seen in both FA and c_L images, and from this small subset of the images one can't tell about tract presence/absence in the rest of the tumor. Dr. Golby found there to be little difference between the images with brightness modulated by FA and c_L, so it seems this choice is not crucial for this application.

Figure 3 shows the raw output of the tractography clustering, where colors are determined by by the clustering algorithm (similar colors appear when tractographic paths map near each other in the high-dimensional space in which clustering is performed). Tractography was initiated in each voxel of a region of interest where cL was above .3. Tractography stopped when cL fell below 0.15. This low stopping value was chosen with the goal of "not leaving out anything" in the tractography. After tractography, which produced over 20,000 paths, a random subset of 10,000 was selected for further clustering and display. The anatomical interpretation of this initial clustering is not clear when all paths are viewed at the same time as in Figure 3.

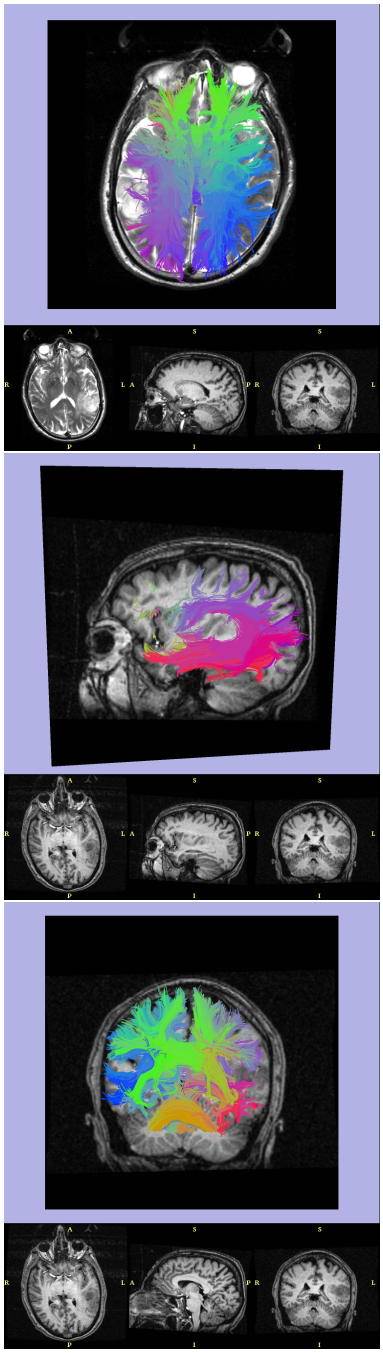

Figure 3: Raw output of whole-brain clustering, shown with axial, sagittal, and coronal images. Each unique color represents a cluster.

After showing the tractography visualization in Figure 3 to Dr. Golby, I returned to the drawing (rendering?) board and attempted to clarify which tracts were passing through the tumor. This is actually more difficult to answer than it sounds, even with so much MRI data, in part due to the fact that it is hard to determine where the tract ends in a tumor. It is possible that edematous tissue contains functioning fibers, but that due to edema the anisotropy in this region is low, which will cause the tractography algorithm to stop tracing. In fact, anisotropy is found to be reduced in in the peritumoral area of both gliomas and metastatic lesions, but the mean diffusion (ADC) is higher at the border of metastatic lesions, apparently due to a higher amount of edema [9]. The anisotropy decrease bordering gliomas is partially attributed to infiltration since there is less edema [9].

Figure 4 shows one possibility for clarifying whether the tract is in a tumor. I have "painted" the tractographic paths with the T2 image volume (keeping the same window/level as the T2 images) in order to transfer its information about tumor boundaries to the tract. In general this method could be used with any available images. I believe this is a useful viewing method, however there are two issues. First the T2 volume could be bright due to edema rather than tumor, and second, the tract tends to "blend in" with the image unless another is placed behind it.

Dr. Golby found this image to be potentially useful, in that the clinician could decide about the tumor boundary intensities using the 2D images, then "paint" the tracts and see whether the tumor intersects. However she informed me that neither the T2 or the FLAIR images differentiate tumor from edema, and that there is interest in diffusion imaging for making this decision. Possibly related to this, note that in Figure 4, in the right image with eigenvector glyphs, there appears to be a region of coherent orientation that was not traced by tractography. This could be due to lower anisotropy in the tumor region that may reflect edema rather than lack of white matter organization, or this region could be infiltrated but still look organized according to the major eigenvectors.

In addition to the attempt to clarify tumor/tract relationships, I labeled the left and right hemisphere using colors matched by structure, in order to facilitate right/left comparisons as suggested by Dr. Golby. This labeling was done manually as an experiment to see if the colors would be useful, and in the future an automatic method would be preferable. Figures 5 and 6 show a subset of the clustered and labeled tracts, with consistent anatomical coloring bilaterally. fMRI activations from a language task are shown in bright yellow. The fMRI task was categorizing nouns as living or nonliving, where patient would respond with either "living" or "nonliving" for each noun. The larger size of the activations on the right side could indicate migration of function to that side.

4.2 Case 2

Patient 2 is 28 years old and presented with seizures. On MRI a lesion was seen in the right insula, extending into the frontal and temporal lobes. The tumor

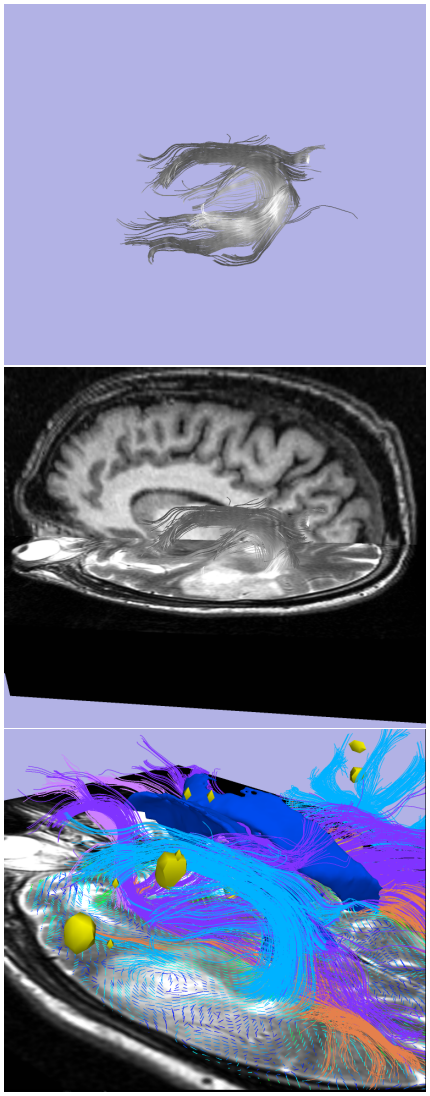

Figure 4: Attempt to clarify whether the arcuate fasciculus passes through the tumor. The left two images show the left arcuate fasciculus, as defined by fiber clustering and labeling, colored using the T2 weighted images. In the middle image the axial T2 is shown to allow comparison of intensities in the tumor and on the tract, while the sagittal T1 is shown for background contrast to make the tract more visible. The bottom image raises the question of if tractography was halted too soon, as there seems to be some organization in the tumor (where the posterior arcuate fasciculus fibers (light blue) meet the tumor). The eigenvector glyphs in the bottom image are colored by anisotropy, with bright blue being highest.

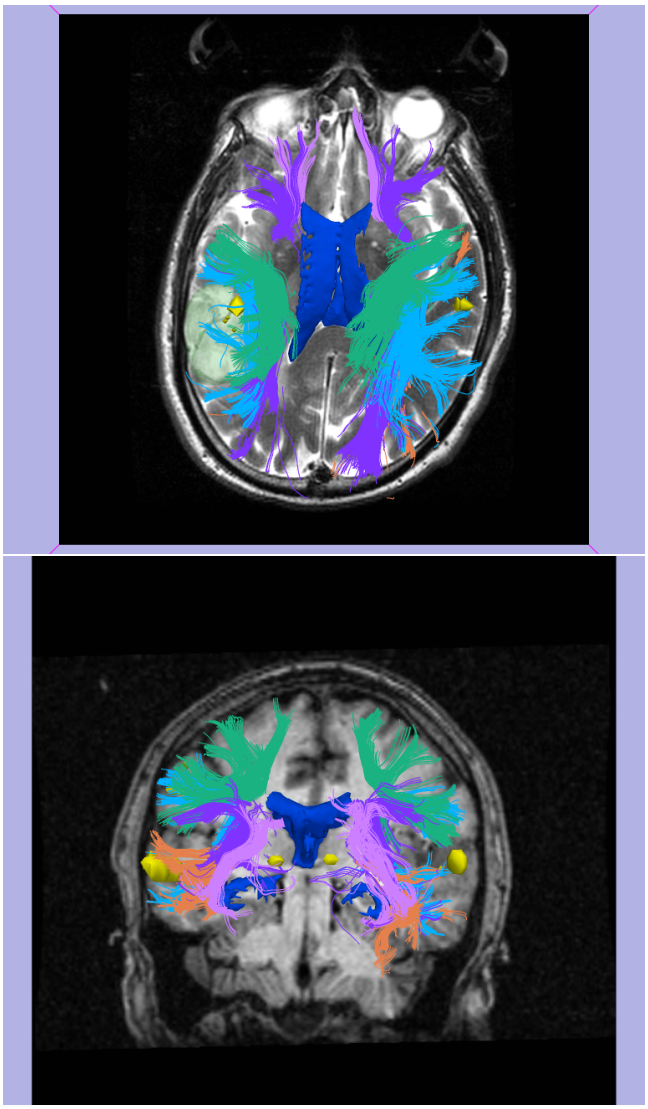

Figure 5: Three-dimensional DTI visualization of patient 1, with consistent coloring on both sides to facilitate left/right hemisphere comparison. Note that the tumor has displaced tracts inferiorly in the coronal view. The colors correspond to anatomy as follows: dark blue, ventricles; light blue, arcuate fasciculus; orange, inferior longitudinal fasciculus; dark purple, inferior fronto-occipital fasciculus; green, unknown name (arcuate or u-fibers); light purple, uncinate fasciculus; and yellow, fMRI language activations. All labeled tracts can't be seen at once, so a subset is shown.

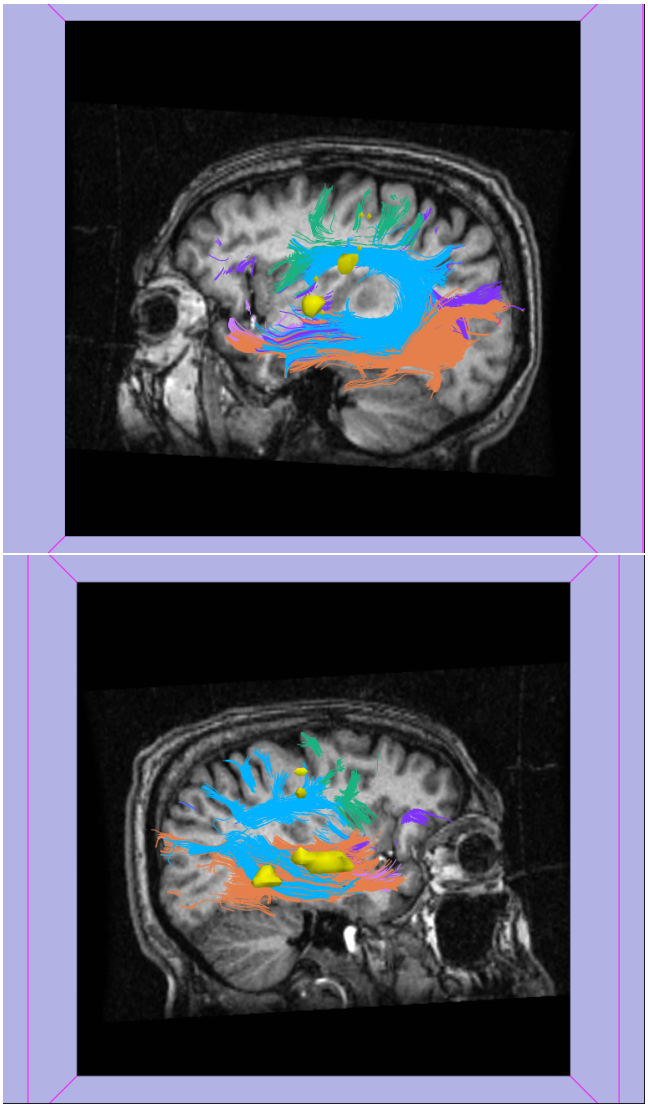

Figure 6: Three-dimensional DTI visualization of patient 1, with consistent coloring on both sides to facilitate left/right hemisphere comparison. The colors correspond to anatomy as follows: dark blue, ventricles; light blue, arcuate fasciculus; orange, inferior longitudinal fasciculus; dark purple, inferior fronto-occipital fasciculus; green, unknown name (arcuate or u-fibers); light purple, uncinate fasciculus; and yellow, fMRI language activations. All labeled tracts can't be seen at once, so a subset is shown.

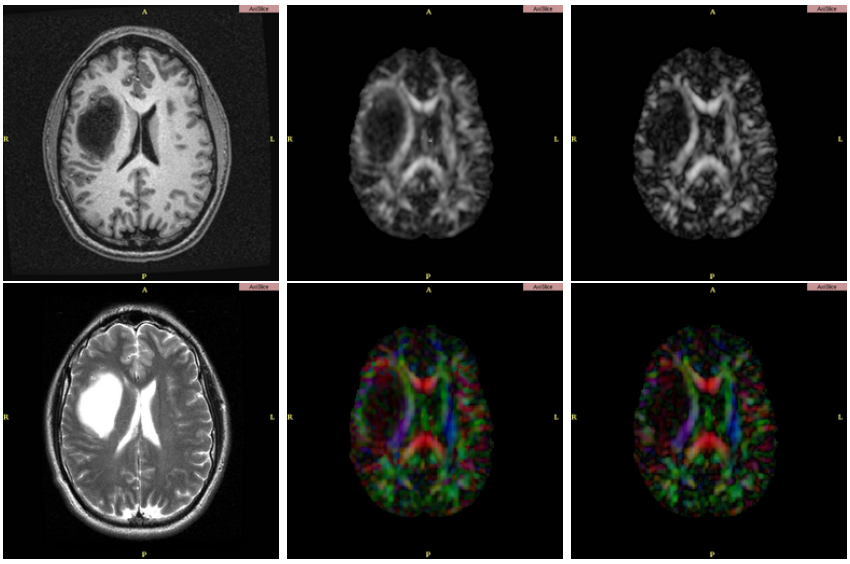

Figure 7: Two-dimensional DTI visualization of patient 2. First row: MPRAGE, FA, c_L. Second row: T2, DTI colormap (brightness by FA), DTI colormap (brightness by c_L)

was classified by pathology as a mixed oligoastrocytoma, WHO Grade II/IV.

In this case I used the same settings as in Case 1 to produce the tractography and create clusters, except that I used a random subset of 8,000 paths instead of 10,000. Interestingly, using the same settings (and the same voxel size and similar number of slices) nearly 50,000 paths were initially produced in this 28 year old subject, versus close to 20,000 in patient 1 (54 years old). This difference may be caused by the overall anisotropy decrease with age, and shows that these thresholds need further investigation.

Figure 7 shows the 2D visualization of the patient, while figures 8 and 9 show the 3D tractography visualization with the same colors as applied in Case 1. The shape of the corona radiata is quite different from left to right, and the uncinate fasciculus curves around the tumor. On the right side, fewer paths belonging to the occipitofrontal fasciculus (dark purple) were found.

5 Conclusion

I have presented the clinical and technical parts of my HST 203 project. During the clinical shadowing part of the project, it became very clear that standard MRI is crucial in neurosurgery. In the technical half of the project, I realized (in fact I was told) that it is not yet clear how DTI should most profitably be employed in neurosurgery. With input from Dr. Golby, I have demonstrated some possible visualization methods that could aid neurosurgical planning. To

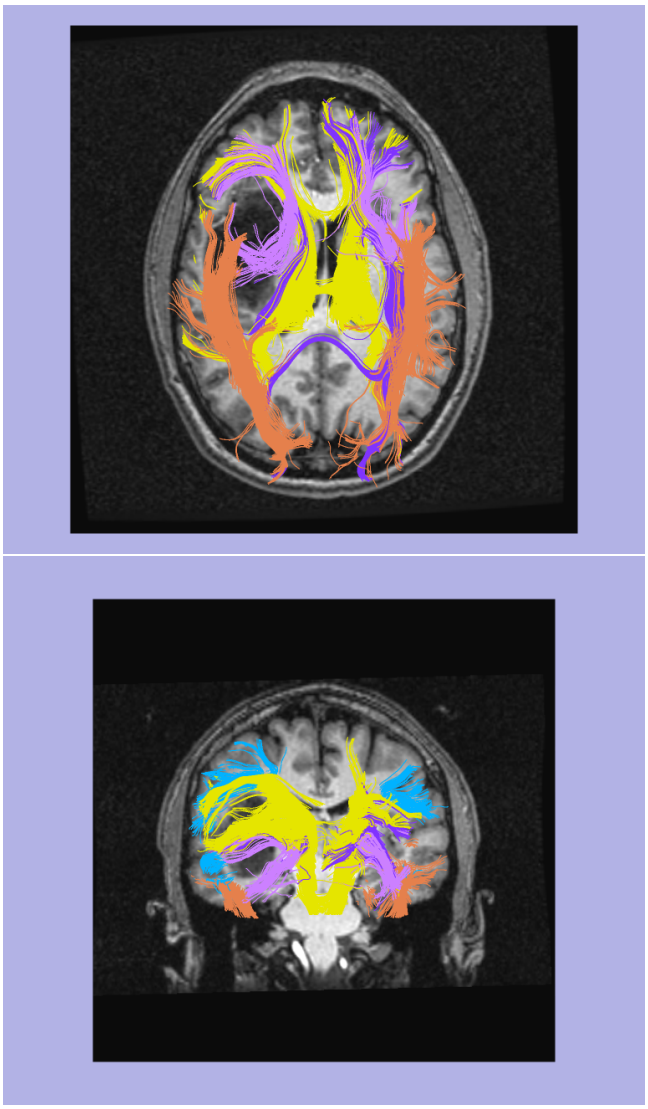

Figure 8: Three-dimensional DTI visualization of patient 2, with consistent coloring on both sides to facilitate left/right hemisphere comparison. The top image is an inferior view, not superior as used for patient 1. The colors correspond to anatomy as follows: light blue, arcuate fasciculus and (on right side) additional fibers bordering tumor; orange, inferior longitudinal fasciculus; dark purple, inferior fronto-occipital fasciculus; light purple, uncinate fasciculus; yellow, corona radiata. Note the differences in the uncinate fasciculus and the corona radiata across hemispheres. There is an error in tractography in the top image, where several paths (dark purple) traverse part of the corpus callosum and part of the occipitofrontal fasciculus.

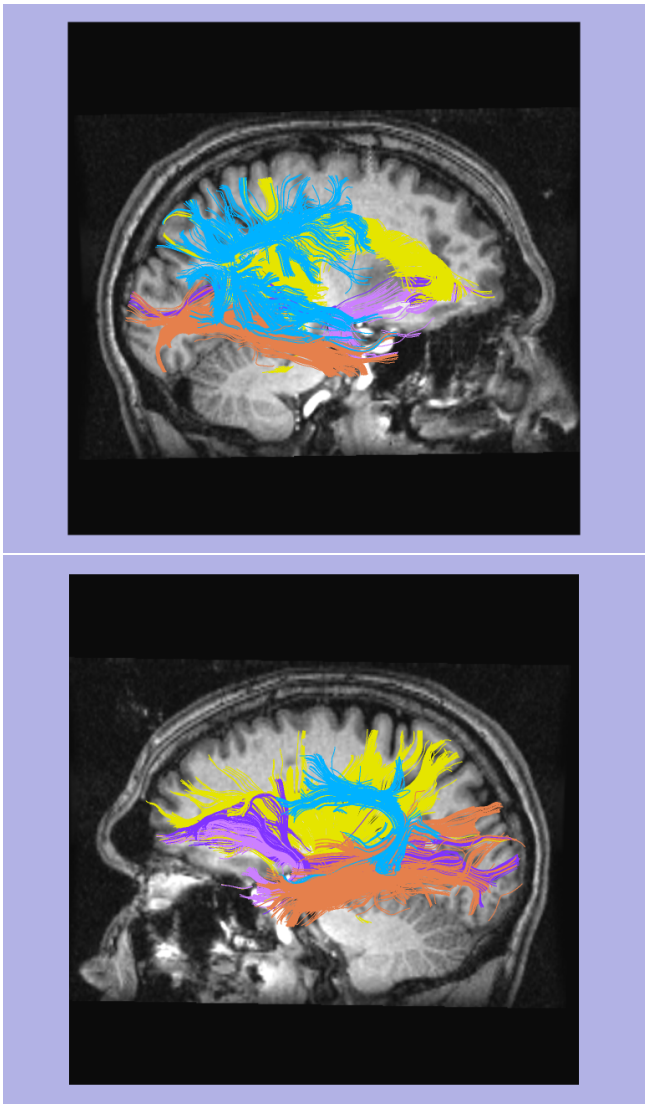

Figure 9: Three-dimensional DTI visualization of patient 2, with consistent coloring on both sides to facilitate left/right hemisphere comparison. The colors correspond to anatomy as follows: light blue, arcuate fasciculus and (on right side) additional fibers bordering tumor; orange, inferior longitudinal fasciculus; dark purple, inferior fronto-occipital fasciculus; light purple, uncinate fasciculus; yellow, corona radiata. Note the differences in the uncinate fasciculus and the corona radiata across hemispheres.

my knowledge, this is the first demonstration of whole-brain patient-specific anatomically labeled tractography for white matter visualization.

6 Acknowledgements

I would like to profusely thank Alex Golby for her amazing explanations of "everything" to do with neurosurgery and the brain, and for her wonderful attitude about having a shadow. This has been an amazing experience. Thanks to Donna Della Iacono for explaining to me about radiotherapy planning and shunt pressure reading, and for showing me how the shunt pressure is set using a magnetic device. Many thanks to the rest of the folks at the neurosurgery clinic, many of whom answered my questions or let me shadow them with a patient. Thanks to the Golby Lab, especially to Stephen Whalen (for giving me data, describing fMRI paradigms, and bringing me to an early morning surgery) and to Ralph Suarez (for teaching me more about fMRI, MEG, and laterality indices). Thanks to Sandy Wells for suggesting the original version of this project and for introducing me to Alex. Finally I would like to acknowledge the HST MEMP Fellowship which has provided fellowship support during this semester.

References

[1] *Brain and Spinal Cord Tumors.* National Institute of Neurological Disorders and Stroke, 1993.

[2] D. B. Ennis and G. Kindlmann. Orthogonal tensor invariants and the analysis of diffusion tensor magnetic resonance images. *Magnetic Resonance in Medicine*, 2005.

[3] B. J. Jellison, A. S. Field, J. Medow, M. Lazar, M. S. Salamat, and A. L. Alexander. Diffusion tensor imaging of cerebral white matter: A pictorial review of physics, fiber tract anatomy, and tumor imaging patterns. *American Journal of Neuroradiology*, 25:356–369, 2004.

[4] M. Kinoshita, K. Yamada, N. Hashimoto, A. Kato, S. Izumoto, T. Baba, M. Maruno, T. Nishimura, and T. Yoshimine. Fiber-tracking does not accurately estimate size of fiber bundle in pathological condition: initial neurosurgical experience using neuronavigation and subcortical white matter stimulation. *Neuroimage*, 25(2):424–429, 2005.

[5] C. Nimsky, O. Ganslandt, P. Hastreiter, R. Wang, T. Benner, A. Sorensen, and R. Fahlbusch. Preoperative and intraoperative diffusion tensor imaging-based fiber tracking in glioma surgery. *Neurosurgery*, 56(1):130–137, 2005.

[6] J. Nolte. *The Human Brain. An Introduction to Its Functional Anatomy.* Mosby, Inc., 2002.

[7] L. O'Donnell and C.-F. Westin. White matter tract clustering and correspondence in populations. In *Conference on Medical Image Computing and Computer-Assisted Intervention (MICCAI)*, 2005.

[8] S. Pajevic and C. Pierpaoli. Color schemes to represent the orientation of anisotropic tissues from diffusion tensor data: application to white matter fiber tract mapping in the human brain. *Magnetic Resonance in Medicine 2000*, 42(3):526–540, 1999.

[9] G. J. Stanley Lu, Daniel Ahn and S. Cha. Peritumoral diffusion tensor imaging of high-grade gliomas and metastatic brain tumors. *American Journal of Neuroradiology*, 24:937–941, 2003.

[10] I.-F. Talos, L. O'Donnell, C.-F. Westin, S. K. Warfield, W. W. III, S.-S. Yoo, L. P. Panych, A. Golby, H. Mamata, S. S. Maier, P. Ratiu, C. R. Guttmann, P. M. Black, F. A. Jolesz, and R. Kikinis. Diffusion tensor and functional MRI fusion with anatomical MRI for image-guided neurosurgery. In *Conference on Medical Image Computing and Computer-Assisted Intervention (MICCAI)*, pages 407–415, Toronto, Canada, 2003.

[11] S. Wakana, H. Jiang, L. M. Nagae-Poetscher, P. C. M. van Zijl, and S. Mori. Fiber tract-based atlas of human white matter anatomy. *Radiology*, 230:77–87, 2004.

[12] C.-F. Westin, S. Maier, H. Mamata, A. Nabavi, F. Jolesz, and R. Kikinis. Processing and visualization of diffusion tensor MRI. *Medical Image Analysis*, 6(2):93–108, 2002.

[13] B. Witwer, R. Moftakhar, K. Hasan, P. Deshmukh, V. Haughton, A. Field, K. Arfanakis, J. Noyes, C. Moritz, M. Meyerand, H. Rowley, A. Alexander, and B. Badie. Diffusion-tensor imaging of white matter tracts in patients with cerebral neoplasm. *J Neurosurg*, 2002.